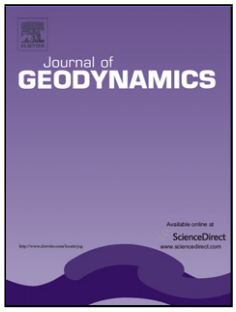

Title: Apulian crust: Top to bottom

Author: Alessandro Amato Irene Bianchi Nicola Piana Agostinetti

PII: S0264-3707(14)00131-8
DOI: http://dx.doi.org/doi:10.1016/j.jog.2014.09.007
Reference: GEOD 1329

To appear in: *Journal of Geodynamics*

Received date: 14-3-2014
Revised date: 9-9-2014
Accepted date: 11-9-2014

Please cite this article as: Bianchi, I., Agostinetti, N.P.,Apulian crust: top to bottom, *Journal of Geodynamics* (2014), http://dx.doi.org/10.1016/j.jog.2014.09.007

Apulian crust: top to bottom

Alessandro Amato, Irene Bianchi, Nicola Piana Agostinetti

Abstract

We investigate the crustal seismic structure of the Adria plate using teleseismic receiver functions (RF) recorded at 12 broadband seismic stations in the Apulia region. Detailed models of the Apulian crust, e.g. the structure of the Apulian Multi-layer Platform (AMP), are crucial for assessing the presence of potential décollements at different depth levels that may play a role in the evolution of the Apenninic orogen. We reconstruct S-wave velocity profiles applying a trans-dimensional Monte Carlo method for the inversion of RF data. Using this method, the resolution at the different depth level is completely dictated by the data and we avoid introducing artifacts in the crustal structure. We focus our study on three different key-elements: the Moho depth, the lower crust S-velocity, and the fine-structure of the AMP. We find a well defined and relatively flat Moho discontinuity below the region at 28-32 km depth, possibly indicating that the original Moho is still preserved in the area. The lower crust appears as a generally low velocity layer (average Vs=3.7 km/s in the 15-26 km depth interval), likely suggestive of a felsic composition, with no significant velocity discontinuities except for its upper and lower boundaries where we find layering. Finally, for the shallow structure, the comparison of RF results with deep well stratigraphic and sonic log data allowed us to constrain the structure of the AMP and the presence of underlying Permo-Triassic (P-T) sediments. We find that the AMP structure displays small-scale heterogeneities in the region, with a thickness of the carbonates layers varying between 4 and 12 km, and is underlain by a thin, discontinuous layer of P-T terrigenous sediments, that are lacking in some areas. This fact may be due to the roughness in the original topography of the continental margins or to heterogeneities in its shallow structure due to the rifting process.

Keywords: crustal structure, receiver functions, Moho, Adria, Apulia, foreland, Apennines, crust

1. Introduction

The Adria microplate is a key element in the present-day evolution of the Mediterranean region, belonging to the Alpine-Hymalayan macro-orogenic process (Figure 1). Such global-scale phenomenon is widely supposed to follow the closure of the Thetys ocean. The final stage of the closure of an ocean should be characterized by the interplay between the subduction of oceanic fragments and the collision/delamination of its continental margins. While the oceanic fragments are thought to sink in the upper mantle, due to their negative buoyancy, the fate of the continental lithosphere is controversial. The deformation of the continental margins leads to its disruption, possibly focused along inherited weak-zones, so that slices of different origin and lithologies are piled up to form the crustal wedge, i.e. the actual mountain chains. It is straightforward that the knowledge of the structure of the involved continental margins is fundamental to model the present-day deformation across the orogens. The Adria microplate represents one of the continental paleo-margins, now fragmented across the Mediterranean region. Unraveling Adria's fine structure and its lateral variations is, thus, a crucial issue to understand what happens when it is subducted/delaminated below the Apennines and the Dinarides.

Many regions of Adria, particularly the foredeeps surrounding it, have been extensively investigated for oil and gas extraction (Mostardini and Merlini, 1987; Nicolai and Gambini, 2007) with seismic lines and deep wells. However, only the upper 7 km (often less) are well known from drillings. Many of these deep wells reached the top of the so-called Apulian Multi-layer Platform (AMP), a thick shallow-water carbonate sequence that developed on the rifted margin in Meso-Cenozoic times. Only rarely boreholes have reached the bottom of the AMP, penetrating Permo-Triassic continental clastic deposits (Patacca et al. 2008; Improta et al., 2000). The top of the AMP below the Apennines and the Adriatic region has been mapped by Nicolai and Gambini (2007). Mariotti and Doglioni (2000) have reconstructed the geometry of the Adria top showing that it dips gently below the belt, with different angles along the foredeep. However, all this information about the Adria structure and geometry did not answer to the question of which part of the AMP has been involved in the tectonic evolution of the belt (Patella et al., 2005; Patacca et al., 2008; Speranza and Chiappini, 2000; Scrocca et al., 2005; Steckler et al., 2008; Chiarabba et al., 2014). Moreover, it is not clear whether the documented lateral heterogenities of the sedimentary cover (Puglia-1, Gargano-1 and Foresta Umbra well-log for the AMP,

Improta et al., 2000; Patacca et al., 2008) could reflect lateral variations in the deep structure. In this situation, uncertainties in the Adria structure lead to very different modeling scenarios for the involvement of the Adria microplate in the orogenic process.

Aim of this study is to reconstruct the Adria crustal structure computing S-velocity profiles retrieved from receiver functions (RF) inversions, in the Apulia foreland region, where the Adria microplate is widely exposed in the Murge and Salento (Figure 1). RF are a widely used tool to investigate the crustal S-wave velocity structure through the analysis of P-to-s converted waves contained in the P-coda of teleseismic events. In this area, the continental margin has not been already affected by significant deformation (i.e. subduction/delamination), and therefore we can retrieve its original seismic structure. Studying the undeformed continental margin allows us to catch both the general features of the Adria Microplate and the small-scale heterogenities, inherited from geodynamic processes that occurred before the closure of the Thetys ocean. In this study, RF are computed from teleseismic data recorded at 12 permanent and temporary seismic stations, with recording period spanning more than 2 years for each station. We focus our analysis on three main issues, namely, the Moho depth, the lower crust structure, and the shallow AMP thickness throughout the study region.

1.1 Geological/Geophysical background

Besides the wide portion submerged below the Adriatic Sea, the Adria microplate includes the Po Plain and Apulia and corresponds to a reduced foreland–foredeep area nearly consumed by the complex orogenic processes occurring along its borders (Patacca and Scandone, 1989; Doglioni et al., 1994; Di Stefano et al., 2009; Piccardi et al., 2011, and references therein). Both the offshore sector and the outcropping area of Adria belong to a foreland basin formed on a lithospheric plate that is flexured between the Apennines, the Alps and the Dinarides-Hellenides chains (Moretti and Royden, 1988; Patacca and Scanodone, 1989; Royden et al., 1987; Mariotti and Doglioni, 2000; Billi and Salvini, 2003). This foreland basin is covered by sedimentary successions that accumulated on the continental margins of Adria since

the early Mesozoic (Channell et al., 1979; D'Argenio and Horvath, 1984; Anderson and Jackson, 1987).

Although there are still different views about its role in the long history of Eurasia-Nubia plate convergence, it is generally accepted that Adria played an important role in the frame of the subduction/collision process of the region, acting as a sort of African promontory (Argand, 1924). Its position, separated from the main Nubia (African) plate by the Ionian sea (a remnant of the Neo-Tethys ocean), would suggest that it is an individual microplate (McKenzie, 1970). However, paleomagnetic data indicate that its long-term motion has been consistent with that of Nubia (Channell, 1996), thus suggesting a substantial continuity across the Ionian sea until recent times. Using GPS data, D'Agostino et al. (2008) suggest that current Adria motion is separate from that of Africa, and propose that active deformation in the central Adriatic is mainly due to the relative motion between Adria s.s. to the north and the Apulia sector to the south. According to this interpretation, the Apulia sector is coherent with the Ionian Sea and the Hyblean block (D'Agostino et al., 2008).

In southern peninsular Italy, Apulia represents the foreland for the southern Apenninic fold-and-thrust belt, below which it dips at low angle (Mariotti and Doglioni, 2000). The AMP is a NW-SE oriented first order paleogeographic unit, consisting of several km thick Upper Triassic-Upper Cretaceous carbonate platform that evolved into a carbonate ramp during the Tertiary. It is approximately 650 km long and at least 175 km wide and played a relevant role in the Apenninic formation (Doglioni et al, 1994; Di Stefano et al., 2009). It extends from the Central Adriatic down to the Patras Gulf where it outcrops in the Ionian Islands. Its western margin is hidden beneath the Southern Apennines thrust units and has not yet been penetrated by any wells (Nicolai and Gambini, 2007).

The deepest part of the Adria crust is much less known, due to the absence of well data below 7 km depth, and the paucity of deep seismic lines. The only deep seismic lines reaching the Adriatic lower crust and Moho are the CROP profiles (Scrocca et al., 2003; Finetti and Del Ben, 2005; Patacca et al., 2008). The Adriatic Sea is underlain by continental crust typically 25–36 km thick, with a maximum of 35–40 km beneath the southern Adriatic basin (e.g., Nicolich, 1981; Dèzes and Ziegler,

2002, Finetti and Del Ben, 2005; Di Stefano et al., 2011; Spada et al., 2013). Lithospheric thicknesses are typically small along the Apulia sector, about 60-90 km, probably related to lithosphere erosion from corner-flow at the Ionian slab edge (Miller and Piana Agostinetti, 2011).

Teleseismic receiver functions were recently used to retrieve Moho depth along the Adriatic side both beneath Italy (Piana Agostinetti and Amato, 2009, and references therein) and Croatia (Stipcevic et al., 2011). As expected in an undeformed margin, the results showed an almost flat Moho, with a depth ranging from about 30 to 35 km, with few anomalous values as high as of 40-45 km (Levin et al., 2003). RF have also been used to reconstruct the whole crustal structure of the Adria microplate in some regions (Levin et al., 2003; Steckler et al., 2008; Piana Agostinetti and Malinverno, 2010; Piana Agostinetti et al., 2011; Di Bona et al., 2011). Retrieved 1D S-velocity profiles depict a fairly horizontally layered crust for the Adria microplate, whose structure becomes more complex structure toward the mountain chain, following the progressive involvement in the orogenic process.

According to different authors, the Adria microplate is dissected by crustal or lithospheric discontinuities that played an important role in the geologic evolution of the Apennines (Di Bucci et al., 2006; D'Agostino et al., 2008; Del Gaudio et al., 2007; Piccardi et al., 2011 and references therein). Such discontinuities define local heterogeneities in the crustal structure of the microplate. More recently, Latorre et al. (2010) have mapped the subsurface structure of the Apulian plate in the foredeep region showing the presence of inherited strike-slip tectonics, consistent with other geologic and seismological studies (Billi et al., 2007). Offshore high-resolution seismic lines have shown that the most recent (Quaternary) deformation is driven by pre-existing (Early Mesozoic?) structures (Ridente and Trincardi, 2006). The ritfing process which leads to opening of an ocean produces a highly heterogeneous margin, with a sequence of deep- and shallow- basins, related to stretching of the crustal blocks involved in the process (e.g. Keen and Beamount, 1990). This would determine variable sedimentation rates which in turn should lead to heterogeneities in the sedimentary cover along the margin (Bosellini, 2004). Small-scale heterogeneities in the AMP have been observed in the Gargano area from borehole litho-stratigraphies. Comparing the well-log of Gargano-1 and Foresta Umbra boreholes,

located 20 km apart, a difference in thickness of about 1.3 km is found for one of the main units of the AMP, i.e. the Dolomia principale formation (Patacca et al., 2008). Older sedimentary cover, i.e. the Triassic Burano formation, displays a less striking variability, being 2.2 km thick at Gargano-1 and more than 2.7 km thick at Foresta Umbra (where the Burano formation has not been drilled to the bottom part).

2.1 Data analysis

We use teleseismic data recorded by permanent stations of the National Seismic Network (Amato and Mele, 2009), and by a few temporary stations installed within the CatScan project (Steckler et al., 2008). The stations are all located in Apulia, right on top of the Meso-Cenozoic carbonatic succession of the Apulian Platform. After visual inspection, we selected good teleseismic events according to their high signal-to-noise ratio; events originated from epicentral distances (Δ) of 30°–100° and with magnitude $Mb > 5.5$ have been recorded at twelve stations (see map in Figure 2) belonging to the Italian National Network of INGV (9), and (2) to the temporal experiment CATSCAN (Steckler et al., 2008). One of the stations (MATE) belongs to the Geofon network. From a total of two thousands recorded events at the 12 stations, we selected a final dataset of about 1200 3-component records, with a minimum of 23 and a maximum of 231 records for single station (see Table 1). Both permanent and temporary stations are equipped with broad-band seismometers. In general, seismic data sets at the temporary stations are of lower quality with respect to those of the permanent stations. This is due to both a shorter recording time that does not allow a full backazimuthal coverage of the teleseismic traces, and a lower signal-to-noise ratio caused by a less accurate installation of the station.

RF data sets are obtained by deconvolution of the vertical from the horizontal recordings into the radial, transverse, and vertical coordinate system, where the radial (R) is computed along the great circle path between the epicenter and the station, positive away from the source, and the transverse (T) direction is calculated 90° clockwise from R. The deconvolution is performed in the frequency domain (Langston, 1979; Ammon, 1991), following the approach proposed by Di Bona (1998). We apply a Gaussian filter ($\alpha = 4$) to limit the frequency band below about 2

Hz (Langston, 1979). The depth-resolution obtained using such cut-off frequency of 2 Hz is approximately 1 km. Due to this limit in the vertical resolution, we cannot expect to resolve completely the finer lithological details of the AMP layering. However, the thickness of the main components of the platform (e.g. the Burano fm.) exceeds 1 km and such layers can be resolved using our RF data-set. At the same time, the limit on the vertical resolution does not allow us to reconstruct a 1D S-velocity profile which contains the same level of details as in a 1D P-velocity profile obtained from the interpretation of sonic-log data (e.g. PUGLIA-1). In this case, we can only discuss mean values of seismic velocities in the main layers of the AMP, losing some of the details contained in the P-velocity profile. High frequency RF data-set are needed to improve the resolving power of this methodology (Leahy et al, 2012).

A representative RF back-azimuthal sweep is displayed in Figure 2a for station AMUR. The RF have been binned to increase the S/N ratio. Bins shown in Figure 2a are obtained by stacking RF for events occurring in the same area. Bins are 20° wide in back azimuth (baz) and 40° wide in Δ, and are computed every 10° in baz, i.e., with a 50% overlapping. In Figure 2a, we plot bins computed for an average Δ = 90° (or Δ = 70°, if Δ = 90° is missing).

For all the stations analyzed in this study (see AMUR for an example, Figure 2a), we find that the transverse components do not show large energy. This is likely due to the relatively flat structure of this stable region that has not undergone relevant deformations in the Meso-Cenozoic, at least. For this reason, in the next sections we discuss only the results of the radial components. We stack the radial receiver functions (RRF) coming from all back-azimuthal directions (Figure 3b) to obtain one stacked RRF that contains information about the isotropic structure underneath the recording station. The standard deviation of the stacked RRF has been calculated by bootstrapping the RRFs ensemble 100 times.

2.2 Inversion Method

In this study we adopt the method developed by Piana Agostinetti and Malinverno (2010), in order to catch the obvious non-uniqueness characteristic of the RRF inverse problem (as seen in Ammon et al., 1990), where single model solutions usually fail. The assumption of horizontal layering, intrinsic in the inversion code, is justified by the simple geologic structure of the undisturbed Apulian plate. The stacked RRF time series is the observed data to solve the inverse problem and gaining inferences about the subsurface seismic structures, together with their estimated standard deviation. A reversible jump Markov chain Monte Carlo (RJMCMC) technique is used to sample the *Vs* parameter space and to retrieve the posterior probability density of the shear velocity beneath a seismic station. The RJMCMC technique does allow to impose very loose a priori information, such that both the *S* velocity and the number of seismic discontinuities at depth are considered as unknowns.

Prior information about the seismic velocity structure was set as follows. The a priori probability distributions of the *S* velocity and *Vp*/*Vs* are considered Gaussian. For these normal distributions, mean and standard deviation (σ) values are kept constant for *Vp*/*Vs* (1.75 and 0.05, respectively), whereas they vary with depth for the *Vs* to account for large-*S* velocity variations expected in the shallow crust, where very different lithologies are present (e.g., clay-sandy sediments and carbonates). The number of interfaces is an unknown itself and can vary between 1 and 30. The maximum number of interfaces is given by the resolution of the RF data set. The maximum depth of the interfaces is given by the length of the portion of RF used in the inversion, 0–30 s, and it is fixed to 60 km in this study. The fit between observed and synthetic RF is computed using a classical χ^2 function. Between two interfaces, both *Vs* and *Vp*/*Vs* is constant. After a burn-in phase of about 25,000 models, which are discarded, the RJMCMC method was used to sample about 175,000 models, from which we computed the a posteriori probability distributions (see Piana Agostinetti and Malinverno, 2010 for details). We ran 95 parallel RJMCMC computations on a linux cluster and obtained an ensemble of about 16×10^6 models. The total CPU time was about 10 hours for each station. The RJMCMC search yields two main results for each seismic station: the posteriori probability distribution (PPD) of the *S* velocity at depth, and the frequency distribution of seismic interfaces at depth sampled during the chain. The PPD of the seismic interfaces at depth broadly indicates how many

isotropic layers are composing the seismic structure beneath each station together with their most probable depths (Figure 2b, panel b).

An example of the technique application is described in Figure 2b for the stacked RRF obtained at station AMUR. The "a posteriori" probability distribution of the *S* velocity at depth can be used to compute a mean *Vs* model and to give a measure of the associated uncertainties (Figure 2b, panel a). The stacked RRF is compared with the synthetic RRF in Figure 2b, panel c.

3. Results

As a result of the inversion, we can look at the velocity profiles derived from the inversion procedure described above with the interfaces distribution in depth, as shown in the example of Figure 2, for station AMUR. The fit between observed and modeled data (upper panel on the right) provides a qualitative estimate of the goodness of the inversion, whereas the dispersion associated with the S velocity values (left panel) tells us how well each value is constrained along depth. The probability density of the interfaces at depth (central panel) roughly indicates the most probable depth-ranges for a seismic discontinuity. As shown in Figure 2 for station AMUR, the fit between observed and modeled data is very good, thanks to the simple 1D structure of the region and to the good teleseismic data available. The interface distribution (Figure 2b) shows that the strongest velocity contrasts below Apulia are those relative to the shallower structure (<10km), and to the Moho discontinuity, at around 30 km depth. This is a feature that we will see in all the stations analyzed in this study, although the variations encountered suggest that lateral heterogeneities do exist.

The results for all the stations are summarized in Figure 3. All the stations share some common features, with some differences witnessing an inhomogeneous structure throughout the Apulian platform. The most evident variations occur in the shallow structure (2-10 km) for most of the stations and are suggestive of a complex evolution of the platform. For all the stations, Figure 3 shows the Vs profile (left), the interface distribution profile (right), and the comparison between synthetic and observed

Receiver Functions (bottom). The fit between observed and modeled RF's is generally very good (Figure 3, lower panels), suggesting that the structure beneath Apulia is well reproduced by a horizontal layer suite, at least at the first order. We describe here the results grouping the stations by area, from north to south:

Gargano region: the two stations in the Gargano promontory (SGRT and MSAG, figure 3a to f) show a similar structure for the upper 10 km, where both have a strong velocity increase at shallow depth (from 0 to 3 km), reaching Vs values of about 4.0 km/s, then two main interfaces between 5 and 10 km depth occur. Between these two interfaces, the S-velocity decreases to about 3.5 km/s at MSAG and about 3.8 km/s at SGRT. The lower velocity is confined in a layer about 2-3 km thick at MSAG, while it slowly increases to mid-crustal velocity in SGRT without any well-defined low-velocity layer. The mid-lower crust is less constrained and shows some difference between the two stations, with SGRT having more interfaces than MSAG. Both stations show a clear, coherent velocity increase between about 26 and 34 km depth, picked around 30, corresponding to the crust-mantle boundary, as will be discussed later. The velocity values along depth have the best resolution at the Moho depth and in the shallowest part of the model. For MSAG, also the region around 10 km depth seems to be well constrained. For both stations, the depth range 10-25 km appears to have the largest uncertainties.

Northern Murge region: stations MRVN, CRBB and, more to the south, AMUR, show similar distribution of interfaces and velocity profiles (figure 3a, panels g to l, and 3b, panels a to c). As before, a strong increase is observed in the top 2-3 km, then S velocities lay between 3.5 and 4.0 km/s in the upper 6 to 8 km, then a velocity inversion right below (Vs as low as 3.3 km/s) occurs. It is worth noting that the portion of upper crust reaching the highest S-velocity value increases its thickness from MRVN to CRBB to AMUR, from 2.5km to 6km thick (depth 2-8km). On the contrary, the low-velocity layer at its base retains almost the same thickness (4km) in all three stations. In the mid-lower crust (12-25 km) there are few interfaces detected, and Vs is around 3.7 km/s (more constant for AMUR and CRBB, slightly higher for MRVN), then a sharp increase around 28-32 km, at the Moho. The two adjacent stations of MRVN and CRBB show a minor hint of velocity discontinuities at 18-20 km depth, below which Vs decreases.

Southern Murge region: station NOCI is located in the middle of the Murge highland whereas MATE and ILCA are located closer to the foredeep (fig. 1). The velocity profiles for the three stations (fig. 3b) are not so similar as in the previous case, with slight differences in the shallow structure: The high velocity layer in the upper crust seems to thicken from MATE (2-8km) to ILCA (2-10km) and NOCI (2-11km), with ILCA showing a low velocity layer in between (Figure 3b). Below, all stations show a low velocity layer as thick as 6-8km at the two western stations, thinning to 4km at NOCI in the highland. The deepest part of the crust is relatively similar among the three stations, with more similarities between MATE and NOCI that have a clear gradient indicating the Moho between 27 and 32 km depth. ILCA shows a gentler gradient in the lower crust, but still with a Moho interface at 30 km depth. It must be said that ILCA was a temporary station and data are less and of lower quality, therefore its results appear to be less constrained: from the comparison between observed and synthetic data, we see a more complex RF waveform between 4 and 7 seconds that we could not model adequately. The uncertainty in the velocity results along depth are small in the top 10 km for MATE and NOCI (larger for ILCA), higher (+/-0.5km/s) in the mid-lower crust, and again very good at the crust-mantle boundary and below.

Salento: three stations are located in Salento, the southernmost tip of Apulia (SRRN, SCTE and NARD) and another one (MESG) is located about 30 km to the north. MESG and NARD have a similar shallow velocity structure, with a strong velocity increase near the surface (0-2 km depth) and a decrease at around 4 km depth. MESG, located close to the eastern margin of the present-day emerged platform, has on average lower Vs values in the whole crust (around 3.5 km/s) compared to the southern stations (Figure 3c). Going deeper, the S velocity remains constant down to 15 km, and it decreases in correspondence of a clear interface below NARD (at 17 km depth), which is less evident at MESG. For both stations the velocity starts to increase again at 26-27 km to reach values of 4.3 km/s at 30-32 km depth. For stations SRRN and SCTE there is no velocity inversion in the shallowest part: below the increase between 0 and 3-4 km depth, there is a constant velocity layer with apparently no interface down to 10-12 km, then a gentle velocity decrease in the whole mid-lower

crust, and the Moho-related positive gradient, between 27km and 34km approximately. Station SCTE also shows a stronger velocity decrease in the lower crust. SRRN was another temporary station of the CatScan experiment, and therefore the data may not be good enough to catch some of the features. The results are very good in terms of associated uncertainties for the three southern stations (NARD, SRRN, SCTE) at almost all depths, excepting the mid-crust at SCTE (Figure 3c). MESG shows higher dispersion at all depths except the Moho level and below.

3.1 Comparison with borehole data

In order to test whether RF data are suited for constraining the thickness and characteristics of the shallow layers throughout the study region, we first compare the RF results at station MRVN (Minervino Murge) with the co-located 7.1 km deep well log of Puglia-1 (Figures 1, 4). In the same Figure 4 we also compare station SGRT results with the stratigraphy of the Gargano-1 and Foresta Umbra deep wells, located nearby. In the latter case, however, the comparison is not so good as for MRVN and Puglia-1 well, due to both the larger distance between SGRT and the deep wells (around 20km), and the more complex structure of the Gargano area with respect to the Apulian Murge highland.

Sonic and stratigraphic logs from Puglia-1 (T.D. 7070 m) and Gargano-1 (T.D. 4853 m) wells have been interpreted by Improta et al. (2000) in order to constrain the structural meaning of two deep seismic discontinuities detected by seismic refraction data at about 6 and 11 km depth. Puglia-1 and Gargano-1 are the only two deep wells of Southern Italy that have crossed the whole Apulia Carbonate Platform, penetrating the sedimentary Paleozoic sediments below the AMP. The 5.9 km-depth borehole in the same Gargano region, Foresta Umbra, did not reach the PT formation (Patacca et al. 2008). The bottom of the Apulia carbonate platform (CP) is relatively well constrained from seismic lines: according to Nicolai and Gambini (2007) the base of the AMP is marked by a typical seismic facies at 2.5-3.0 s (twt) below its top, in agreement with well data, and corresponding to 6-9 km, approximately. A critical issue in the interpretation of the Apulia structure is related to what underlies the CP, likely the Paleozoic crystalline basement (Patacca et al., 2008). This unit is not

accessible in many deep wells, and seismic data (commercial Near Vertical Reflection NVR seismic lines, CROP deep crustal reflection profiles, wide-angle DSS profiles) depict the base of the sedimentary cover but cannot constrain the structure and thickness of the underlying basement (Improta, 2000).

The Puglia-1 well penetrates: (1) Early-Cretaceous wackestone-packstone, (2) Cretaceous–Liassic limestones, dolomitic limestones and dolostones from about 1000 m to 3535 m, with P velocities in the range 6.0–6.2 km/s below 1km depth; (3) dolomites of uncertain age (scarce or no recovery of cuttings) from 3535 to 5000 m, characterized by higher velocities; (4) Triassic dolomites and anhydrites of the Burano formation from 5000 to 6112 m, both with velocities in the range 6.4–6.7km/s; and finally (5) Lower Triassic–Permian siliciclastic deposits referrable to the Verrucano formation from 6112 to the final depth (7070 m) (Figure 4), showing a considerable velocity decrease down to 5.0–5.5 km/s (Improta et al., 2000). The comparison with our RF results is surprisingly good, keeping in mind the 1km resolution of our results: we detect a strong increase in S velocity in the upper 1-2 km, then from 2 to 5 km depth the Vs computed by RF is around 3.2-3.7 km/s (in agreement with Vp of 6.0-6.7 km/s measured in the well). Our RF data are consistent with a layered structure of the Apulian Platform, with a main interface at around 3 km depth, that corresponds with the passage from Cretaceous-Jurassic limestones to dolostones at greater depth, as found in Puglia-1 well. The uncertainty on Vs values in these layers are quite small, around 0.25 km/s. Going deeper, our posterior mean model predicts a velocity decrease between 5 and 6 km depth, in good agreement with what found in Puglia-1. The depth range of such decrease in the posterior mean model is slightly biased by the presence of a bimodal posterior probability distribution on the Vs parameter at such depth (Figure 4a, panel (g)). This fact is due to the intrinsic trade-off between depth and S-velocity in the RF. Higher frequency RF should be used to reduce the resolution to less than 1 km.

The seismo-stratigraphic succession described for Puglia-1 is confirmed by Gargano 1 well (Figure 5), located 90 km north of the former (Figure 1) in a region characterized by higher elevation and strong strike-slip tectonics. According to Improta et al. (2000) the only relevant difference between the two wells is the thickening of the high velocity Burano evaporites from 1.1 to 2.0 km. Also note that in the Gargano region

there are two deep wells (Gargano-1 and Foresta Umbra-1) located close to each other, but with a remarkable difference in the thickness and structure of the Triassic anhydrites (the Burano Formation). This could be an indication of inhomogeneous crustal setting at the time of the marine deposition, possibly due to the proximity of a ramp of the platform, and/or of subsequent tectonic activity in the region. Figure 4 also shows that the total thickness of the AMP is lower in Gargano-1 than in Puglia-1.

From these observations, we define four criteria that are used to interpret the posterior mean S-velocity profile of each station, starting from the free-surface and going to almost 15km depth. First, (1) the shallowest layer is composed of (possibly intraclastic) wackstone/packstone, where lower S-velocity, with respect to the deeper layer, can be induced by higher-porosity/smaller-grain-size or (more likely) different cementation (Brigaud et al., 2010). Moreover, the stations deployed in the Bradanic foredeep (i.e. ILCA and MATE) have Quaternary deposits near the surface. (2) The second layer represents the Lower-Jurassic limestone of the AMP, where the S-velocity increases with respect to the first layer, but does not reach the Burano fm S-velocity (Vs>3.8km/s, Trippetta et al., 2010). (3) The third high S-velocity layer indicates the presence of the Burano fm, which includes both evaporites and dolomies (Vs>3.8 km/s). Finally, (4) the silico-clastic layer is considered, if below the Burano fm. a low S-velocity layer is found with respect to the Middle crust (i.e. if the S-velocity decreases with respect to both the Burano fm and the Middle crust). This criteria is considered only if the depth of the bottom of the S-velocity layer does not exceed 12 km (i.e. the Silicio-calstic layer can not reach more than 12km depth). It is worth noticing that, while these criteria can provide a very useful first-order guidance to the interpretation of the S-velocity profile in the study area, the association between S-velocity and lithology is not unique. Geological/geophysical information is needed to discriminate between different plausible lithologies sharing similar S-velocity, and different lithological stratigraphy cannot be excluded using solely the analysis of a Receiver Function data-set. The criteria delineated above are used to associate the S-velocity profiles to the lithological units in Figure 5.

Interpretation and discussion

In this section, we discuss the results of the RF inversion and interpret them in terms of lithological discontinuities and rock properties. As we have seen in the previous section, there are several common features among all the stations, that are, from top to bottom: a) the upper 10-12 km of the crust, characterized by strong layering and velocity jumps, with one relevant velocity inversion that is found at almost all the stations; b) the middle and lower crust (15 to 30 km depth) with few velocity discontinuities, and, in some cases, a low-velocity zone in the 20-25 depth range; c) the velocity discontinuity at around 30 km depth, corresponding to the crust-mantle boundary, i.e., the Moho.

The shallow structure.

We know from outcrops and deep wells that the shallow crustal structure of Apulia is characterized by Meso-Cenozoic (M-C) platform deposits, mostly composed by limestones, dolostones and evaporites, underlain by Permo-Triassic (P-T) clastic continental rocks. This sedimentary suite lies above a Hercynian basement, drilled in at least one deep well in northern Adriatic (Assunta-1, near Venice), and constituted by metamorphic and probably intrusive rocks. This basement has been reconstructed by seismic profiles in various spots of the Adriatic plate, mostly offshore. Some deep wells drilled in the Apulian offshore (Amanda-1, bottom depth 7.3 km) and onshore (Puglia-1, bottom 7.1 km), did not cross the metamorphic basement but stopped in the overlying P-T sediments, that mark the onset of the rifting phase of the Neo-Tethys.

The sedimentary succession deposited in M-C times displays some relevant velocity jumps, as shown by the Puglia-1, the Gargano-1 and the Foresta Umbra deep wells (Improta et al., 2000; Patacca et al., 2008), and by our RF results (Figure 4). Here we discuss (a) the thickness of the AMP, (b) the presence and nature of one or more layers in the AMP, and (c) the presence and thickness of the P-T sediments at the base of the AMP; d) the presence of the metamorphic basement.

In general, we find significant variations in the top part of the velocity profiles (Figure 4), attributed to the AMP structure, including M-C carbonates and P-T sediments. For P-T sediments, this can be related to the continental deposition, i.e., no deposition and/or high rate of erosion on structural highs. For M-C deposits, the variations can be

interpreted in terms of faster/slower deposition/subsidence/erosion rate of the platform, and can be hints for tectonic discontinuities dissecting the platform.

Looking at the AMP distribution throughout the whole Apulia region (Figure 5), we find a general increase of the M-C platform sediments thickness moving from North to South. In this figure we have interpreted the velocity profiles, attributing the along-depth layering to the geologic units, as explained in the previous section. The northernmost stations, including Gargano and northern Murge, show an AMP thickness of 4-6km, in agreement with the deep wells stratigraphy, as discussed before. Moving to central Apulia (stations AMUR, MATE, ILCA, NOCI) the high Vs layers of the AMP are as thick as 8-10km, whereas the southternmost stations SRRN and SCTE show even larger thickness (11 km). In between, both MESG and NARD have a different velocity profile in the upper crust, with a velocity reduction below 5 km that suggests a thinner AMP in this region, and the presence of P-T sediments just below it. This variation can be interpreted in terms of a dissected Apulian platform beneath Murge and Salento, in correspondence with the lowered topography of the region in between (Figure 1). An alternative explanation for station MESG, located close to the Adriatic coast, is suggested by a long commercial seismic line (n. D82-59-55, Improta, personal communication) running for 150km along the Apulian coast, a few km offshore. This line shows a clear thickening of the AMP from NW to SE, from 2.4s TWT to 3.4s TWT (corresponding approximately to a 2-3km thickening). This is in agreement with the general thickening that we observe from RF velocity profiles. Moreover, since the D82-59-55 line runs in a region of lateral ramp of the platform, we can argue that the central part of the AMP is likely even thicker, in agreement with our results. The same line, as well as other commercial and scientific seismic lines shot in the area, also show the presence of normal faults dissecting the continuity of the Apulian platform. These faults, interpreted as inherited faults from the Mesozoic rifting phase, can explain the different thickness of the AMP found in our RF data. According to Nicolai and Gambini (2007), a major plate rearrangement in Middle-Upper Cretaceous times converted part of the Tethyan realm from an extensional to a compressional regime. Since the Middle Cretaceous, large parts of these platforms were partly exposed and extensively karstified, and during the Upper Cretaceous a few intra-platform basins have developed in the Apulian Platform area (Nicolai and Gambini, 2007). This could explain the difference that we find in stations

not so far from each other, particularly in terms of velocities at the same depth level, in the AMP. For instance, station ILCA (figure 4) shows a double layering of the top 10-12 km, with two velocity reversals at 2km and 10km depth. This could be due to a heterogeneous platform suite, with alternance of high velocity limestones/dolostones and low velocity ramp or basinal units. Not far from ILCA, MATE (figure 2) shows a similar structure, with a slightly thinner platform (8km) and a less pronounced (but still visible) velocity decrease at around 4-5 km depth. An alternative explanation for the low velocity in the AMP structure at ILCA, not far from the Apenninic foredeep, is the presence of faults and fractures that developed during the flexural subsidence of Adria while approaching the foredeep.

Below the stack of AMP high Vs layers, we find a velocity inversion beneath most of the stations, that we interpret as the P-T clastic sediments following the results of Puglia-1 well (Improta et al., 2000). The sonic log available for the well shows a clear Vp decrease as high as -2 km/s at 6km depth, in correspondence of the base of the M-C platform deposits (figure 5). This low velocity layer is well evident from RF results in most of the northern stations, such as MSAG (6-8km), MRVN (6-9km), CRBB (7-10km), a little bit deeper in central Apulia, as at AMUR (8-12km), NOCI (11-14km), MATE (8-14km). However, the low velocity region is more uncertain in the south (SRRN, SCTE, NARD) where the thicker AMP layers (12km) overlie a more homogeneous low velocity region (Vs=3.7-3.8 km/s) down to lower crustal depths. We hypothesize that in southernmost Apulia the AMP developed directly above the Hercynian metamorphic/crystalline basement.

According to our results, we can constrain the thickness of the Permo-Triassic clastic sediments to as much as 3-4 km, with the exception of MATE that shows greater thickness. This finding is in agreement with what hypothesized by Patella et al. (2005) and Finetti and Del Ben (2005), based on magnetotelluric analyses and seismic profiles, respectively, and disagree with the hypothesis of a thicker formation of continental sediments postulated by Patacca et al. (2008). In particular, Patella et al. (2005) image a thin (1 to 3-4 km) conductive layer of clastic sediments separating the AMP from the high resistivity crystalline basement. It seems that the conductive layer is thinner moving southeastward (the profile in Patella et al., 2008, runs north of Puglia-1 well). Combining this evidence with our results of no such clastic sequence in southeastern Apulia (Figures 4 and 6), we may hypothesize that the rifting process

dissecting Africa from Apulia and forming the Neo-Tethyan basin has progressed asynchronously. In some areas, such as the Salento area in SE Apulia, the absence of the P-T clastic sequence may indicate an uplift episode or an old erosional event.

The middle-lower crust.

To investigate what happens at greater depth, we plot in Figure 6 all the Vs profiles from the sea level to the bottom of the model, dividing the stations in the four geographical groups described above. As noted before, there is a general good agreement among most of the stations, with some differences also at intermediate crustal depth. In our RF inversion, the main characteristics of the Vs profiles in the middle crust are: (1) a velocity increase for most of the stations at 10-15 km depth (below the P-T sediments, where present), (2) an almost constant Vs between 15 and 22 km depth, and (3) a decrease in Vs below 22-25 km for some stations. Then the Vs increases more or less gradually down to 30 km, in correspondence of the crust-mantle boundary. A gradational change to mantle velocity should suggest a layered lower crust, however, the trade-off between Vs and depth does not allow to completely resolve sharp boundaries using this RF inversion technique (Piana Agostinetti and Malinverno, 2010). The interface with the velocity increase below 10km is visible only at some of the stations, particularly those in northern and central Apulia (figure 6). Based on seismic reflection profiles (Scrocca et al., 2003; Finetti, 2005) and MT data (Patella et al., 2005) we interpret this interface as the top of the Paleozoic crystalline basement. The lateral variations along the region, even more evident in the seismic reflection data, could be due to different characteristics of the mid-crustal layering.

Going deeper in the middle-lower crust, some of the stations show the presence of velocity discontinuities around 20 km, but with large variations (Figure 3), as in NARD, MRVN, and to some extent SGRT, CRBB, SCTE. These discontinuities are always marked by a velocity decrease below that depth, suggesting a low velocity lower crust (Vs as low as 3.7-3.8km/s). The low velocity lower crust is particularly evident in the Gargano area below 24km (Figure 6, left panel). Other stations where this 20-km-depth discontinuity is not visible show more diffuse layering just above the Moho (25-30 km depth range, e.g. MSAG, AMUR, MESG). In any case, there are

610 hints of a layered lower crust below 20 and 30 km depth, with Vs increasing from less
611 than 4.0 km/s to 4.3km/s.
612
613 The thickness and composition of the middle and lower crust in the Adriatic region is
614 still largely unknown. Commercial seismic lines do not reach depth larger than 10 km
615 or, if they do, they have not enough resolution to constrain the deep layers. Some data
616 come from the CROP profiles, deep crustal seismic lines performed for scientific
617 research. Some of the offshore lines allow us to define some constraints for the deep
618 structure. Finetti and Del Ben (2005) suggest a thickness of the "UC" (upper crust
619 without sediments) of about 4 s TWT (about 12km) in the offshore south of Salento,
620 and 2.5-3 s TWT (about 8-10km) for the lower crust. According to these authors, both
621 north of Gargano and south of Salento, the whole crustal stack is dissected by strike-
622 slip and normal faults that determines variations on thickness of the crustal layers. In
623 addition, both Finetti and Del Ben (2005) and Patella et al. (2005) propose the
624 presence of large reflective magmatic bodies at mid-crustal depth in the Apulian plate.
625
626 Data from deep seismic reflection lines onshore (CROP04 and CROP 11, Patacca et
627 al., 2008) cannot constrain well the structure of the mid-lower crust, because data
628 quality is low at these depths except in some limited spots. However, they reveal a
629 thick band of dominantly sub-horizontal reflectors interpreted as lower crustal
630 layering. In particular, Patacca et al. (2008) find two main layers in the lower crust,
631 the shallowest of which (between 9.7s and 10.7s TWT, corresponding roughly to 25-
632 30km below the belt) has a strongly layered seismic fabric, and below (but still above
633 the Moho), scattered sets of parallel reflectors with variable amplitude and frequency.
634 The two lower crustal layers might correspond in our RF Vs model to the peaks in the
635 probability density plots of discontinuities that we described above. The lower layers
636 of Patacca et al. (2008) would correspond to our "layered" zone between 20 and 28km
637 depth, where we find no well-defined Vs discontinuities and generally low Vs.
638 The lower crust is believed to consist of metamorphic rocks in the granulite facies;
639 however, the composition of the deep crust remains the largest uncertainty while
640 determining the crust's overall composition. This is due to the large compositional
641 differences between granulites terrains observed at the surface (mainly of felsic
642 composition) and the lower crustal xenoliths (in which mafic rocks dominate) (Rudnik
643 and Fountain 1995). The retrieved average velocities of the lowermost (15-26 km

644 depth) layers of our velocity models are more typical of felsic composition of the
645 lower crust (Rudnik and Fountain 1995, Wedepohl, 1995). Often the seismic structure
646 of the lower crust appears highly reflective due to the presence of subhorizontal
647 layering, either spread in the entire lower crust or confined to its upper and lower
648 boundaries (see Mooney and Brocher (1987) for a review). This latter case appears to
649 be more consistent with our results for the Apulia crust. The origin of reflections
650 includes acoustic impedance contrasts due to solidified igneous intrusions, molten or
651 partially molten bodies, fine-scale lithologic layering of metamorphic rocks, or
652 localized ductile shear zones (Mooney and Meissner, 1992). Anyway, the absence of
653 layering that we encounter in the study area does not imply the absence of
654 compositional (or structural) variability, since many rock types have similar acoustic
655 impedance, or the presence of small-scale heterogeneities that may cause destructive
656 interference.
657
658 The presence of a low S-velocity zone within the lower crust, together with
659 substantial layering at the same depth level, might be related to the fluid-filled layer
660 found in the middle lower crust north of the Apulian region (Chiarabba et al., 2014a).
661 The presence of such layer could indicate the occurrence of a change in the crustal
662 rheology which promotes the post-subduction delamination of the continental
663 lithosphere. Delamination of the continental lower crust has been observed, after
664 subduction episodes, along the central Mediterranean region (Piana Agostinetti et al.,
665 2011; Chiarabba et al. 2014b). Such process involves the former passive continental
666 margin, when the oceanic plate has been completely subducted, and evolves from the
667 negative buoyancy of the continental lithosphere with respect to the underlying upper
668 mantle. Thus, a weak zone within the continental middle-lower crust would guide the
669 sinking of the continental lithospheric mantle (Gogus and Pysklywec, 2008).
670
671
672
673 *The Moho.*
674 As described in the previous sections (Figures 3 and 5) all the seismic stations show a
675 clear velocity jump around 30 km depth. In the velocity-depth profiles, this jump
676 appears like a relatively gradual transition: S velocity increases from ~25 to 30-32 km
677 depth, with values ranging from ~3.5 km/s to 4.2-4.4 km/s. This result is in good

agreement with previous estimates (Table 1), in particular with the results from the H-k stacking method (Zhu and Kanamori, 2000) used in Piana Agostinetti and Amato (2009) (Figure 1). There is also a good agreement of our results with the Moho depth estimates based on CROP and other seismic sections summarized by Finetti (2005). For the Apulia region, Finetti (2005) finds a Moho depth around 30 km or less in the Gargano, and a gradual thickening to 34 km southeastward. Di Stefano et al. (2011) also find a similar smooth trend in southeastern Italy. However, we note that the Moho estimates in these studies are obtained from interpolation of off-shore seismic profiles, some smooth constraints from gravity modeling and the published RF estimates, which were not many in the past years.

In order to obtain our best estimate for the crust-mantle boundary, we extracted the Moho depth from the maximum of the histograms of the layer distribution from the Rj inversion. We computed the mean and the standard deviation of the Moho depth from the histograms in the 20-40 km depth range (Figure 7). Moho depth ranges from 28 to 32 km, with uncertainties of ± 2km. According to our results, the Apulian Moho is rather flat and tends to thicken gently in the southeastern region (Salento) where we find values around 32km. Also beaneah Gargano we find values slightly larger than the average, i.e., 31km. As described above, most of the stations exhibit a strong layering just above the Moho, with increasing velocities.

The regular geometry of the Apulian Moho is very peculiar for peninsular Italy. A flat Moho is found only in two regions (Piana Agostinetti and Amato, 2009; Di Stefano et al., 2011, and references therein), namely the Apulian foreland and the Tyrrhenian back-arc region. This is consistent with the geological setting of Apulia and its stability as a foreland area in the last tens of millions years. Due to the vicinity of the Ionian oceanic basin and the transitional character of passive margins, we could expect to see the rifting phase imprinted in the present Moho structure (i.e. undulations in the Moho topography). This is not the case, and we speculate that it might be a Moho newly formed after the rifting phase that dissected the Paleozoic Hercynian structure, possibly accompanied with magmatic underplating (Eaton, 2006).

Conclusions

In this paper, we reconstruct the 1D S-wave velocity profiles of the Adria microplate using data from 12 broadband seismic stations deployed along the Apulian sector of the microplate. Overall, our results are in agreement with previously published Moho depth maps and locally with litho-stratigraphy from deep well drilled in the area. Through the comparison with two deep wells located near our seismic stations, we have verified that our RF results have enough resolution to constrain the crustal structure of the region. We identify three main findings in our results: the fine structure of the Apulian Multi-layer Platform, the lower crust seismic structure, and the Moho depth estimates.

1. The structure of the AMP displays small-scale heterogeneities in the region, with a thickness of the carbonates layers that varies between 4 and 12 km, and the absence of the Permo-Triassic sediments at some locations, suggesting the direct emplacement of the carbonate sedimentation on the Hercynian basement.
2. A "fine layered" structure seems to characterize the lower crust, especially in the depth range directly above the crust-mantle boundary. The S-wave velocity in the lower crust generally displays low value, possibly indicating a change in crustal rheology and the depth level where post-subduction continental delamination might develop.
3. Our Moho depth estimates are well constrained by the data and are in general agreement with previous studies, offering more details in some areas. We find very consistent values oscillating between 28 and 32 km depth throughout the region. The hypothesized crustal thickening from NW to SE is not confirmed by our data. Even if the two southernmost stations have the largest values (32km), also the two stations in the Gargano area have similar values (31km).

Acknowledgements

NPA research is conducted with the financial support of Science Foundation Ireland

747 & the Marie-Curie Action COFUND under Grant Number 11/SIRG/E2174. We thank
748 Luigi Improta for useful discussions. We thank the staff of the INGV Centro
749 Nazionale Terremoti for network maintainance and data distribution.
750
751
752

753 **References**
754
755 Amato, A., Mele F. M. (2008) Performance of the INGV National Seismic Network
756 from 1997 to 2007, Annals of Geophysics, vol. 51, no.2/3, 417-431, 2008.
757
758 Ammon, C., G. E. Randall, and G. Zandt (1990), On the non-uniqueness of receiver
759 function inversions, J. Geophys. Res., 95, 15,303–15,318.
760
761 Ammon, C. (1991), The isolation of receiver effects from teleseismic *p* waveforms,
762 Bull. Seismol. Soc. Am., 81, 2504–2510.
763
764 Anderson, H.J. & Jackson, J. (1987) Active tectonics of the Adriatic region. Geophys.
765 J. Roy. Astron. Soc., 91, 937-987.
766
767 Argand, E. (1924), La tectonique de L'Asie, paper presented at the 13th Congress,
768 Geol. Int., Brussels.
769
770 Billi, A., Salvini, F. (2003) Development of systematic joints in response to flexure-
771 related fibre stress in flexed foreland plates: the Apulian forebulge case history, Italy.
772 Journal of Geodynamics, 36, 523-536.
773
774 Billi, A., R. Gambini, C. Nicolai, and F. Storti (2007), Neogene-Quaternary
775 intraforeland transpression along a Mesozoic platform-basin margin: The Gargano
776 fault system, Adria, Italy, Geosphere, 3(1), 1–15, doi:10.1130/GES00057.1.
777
778 Bosellini, A. (2004), The western passive margin of Adria and its carbonate
779 platforms, Special Volume of the Italian Geological Society for the IGC 32 Florence-
780 2004, 79-92.
781
782 Brigaud, B., B. Vincent, C. Durlet, J.-F. Deconinck, P. Blanc, A. Trouiller (2010),
783 Acoustic properties of ancient shallow-marine carbonates: effects of depositional
784 environments and diagenetic processes (Middle Jurassic, Paris basin, France), Journal
785 of Sedimentary Research, 2010, v. 80, 791–807, Research Article, DOI:
786 10.2110/jsr.2010.071
787
788 Channell, J. E. T. (1996), Palaeomagnetism and palaeogeography of Adria, in
789 Palaeomagnetism and Tectonics of the Mediterranean Region, edited by A. Morris
790 and D. H. Tarling, Geol. Soc. Spec. Publ., 105, 119–132.
791
792 Channell, J. E. T., B. D'Argenio, and F. Horvath (1979), Adria, the African
793 promontory in Mesozoic Mediterranean paleogeography, Earth Sci. Rev., 15, 213–
794 292.
795
796 Chiarabba, C., P. De Gori, D. Latorre, and A. Amato (2014a), Crustal structure in the
797 area of the 2002 Molise earthquake: Clues for the evolution of the southern
798 Apennines, Tectonics, 33, doi:10.1002/2013TC003406.
799
800
801

802 Chiarabba, C., G. Giacomuzzi, I. Bianchi, N. Piana Agostinetti, J. Park (2014b) From
803 underplating to delamination-retreat in the northern Apennines, Earth and Planetary
804 Science Letters, 403, 108-116.
805
806 Consiglio Nazionale delle Ricerche (1983) Structural Model of Italy and Gravity map.
807 Quaderni della Ricerca Scientifica, N. 114, vol. 3. S.E.L.C.A., Florence, Italy.
808
809 D'Agostino, N., Avallone, A., Cheloni, D., D'Anastasio, E., Mantenuto, S. and
810 Selvaggi, G. (2008), Active tectonics of the Adriatic region from GPS and earthquake
811 slip vectors, J. Geophys. Res., 113, B12413, doi:10.1029/2008JB005860.
812
813 D'Argenio, B., Horvath, F. Some remarks on the deformation history of Adria, from
814 the Mesozoic to the Tertiary. Annales Geophysicae 1984; 2:143-146.
815
816 Del Gaudio, V., P. Pierri, A. Frepoli, G. Calcagnile, N. Venisti, and G. B. Cimini
817 (2007), A critical revision of the seismicity of the Northen Apulia (Adriatic
818 microplate? Southern Italy) and implications for the identification of seismogenic
819 structures, Tectonophysics, 436, 9–35, doi:10.1016/j.tecto.2007.02.013.
820
821 Dèzes, P. and Ziegler, P.A., 2004. Moho depth map of Western and Central Europe.
822 EUCOR-URGENT home page: http://www.unibas.ch/.
823
824 Di Bona, M. (1998), Variance estimate in frequency-domain deconvolution for
825 teleseismic receiver function computation, Geophys. J. Int., 134, 634–646.
826
827 Di Bona, M., F. P. Lucente and N. Piana Agostinetti (2008), Crustal structure and
828 Moho depth profile crossing the central Apennines (Italy) along the N42° parallel, J.
829 Geophys. Res., 113, B12306, doi:10.1029/2008JB005625.
830
831 Di Bucci, D., A. Ravaglia, S. Seno, G. Toscani, U. Fracassi, and G. Valensise (2006),
832 Seismotectonics of the southern Apennines and Adriatic foreland: Insights on active
833 regional E-W shear zones from analogue modeling, Tectonics, 25, TC4015,
834 doi:10.1029/2005TC001898.
835
836 Di Stefano, R., E. Kissling, C. Chiarabba, A. Amato, and D. Giardini (2009), Shallow
837 subduction beneath Italy: three-dimensional images of the Adriatic-European-
838 Tyrrhenian Lithosphere system based on high-quality P-wave arrival times, J.
839 Geophys. Res., 114, B05305, doi:10.1029/2008JB005641.
840
841 Di Stefano, R., I. Bianchi, M. G. Ciaccio, G. Carrara, and E. Kissling (2011), Three-
842 dimensional Moho topography in Italy: New constraints from receiver functions and
843 controlled source seismology, Geochem. Geophys. Geosyst., 12, Q09006,
844 doi:10.1029/2011GC003649.
845
846 Doglioni, C., Mongelli, F. & Pieri, P. (1994) The Puglia uplift (SE Italy): an anomaly
847 in the foreland of the Apennine subduction due to buckling of a thick continental
848 lithosphere. Tectonics, 13, 1309-1321.
849

Eaton, D. W. Multi-genetic origin of the continental Moho: insights from LITHOPROBE (2006), Terra Nova, 18, 34–43, doi: 10.1111/j.1365-3121.2005.00657.x

Finetti. I. (2005). Depth contour map of the Moho discontinuity in the Central Mediterranean region from new CROP seismic data. In: CROP PROJECT: deep seismic exploration of the Central Mediterranean and Italy, p. 597-606. I. Finetti ed., Elsevier.

Finetti. I., and A. Del Ben (2005). Crustal tectonic-stratigraphic setting of the Adriatic Sea from new CROP seismic data (2005). In: CROP PROJECT: deep seismic exploration of the Central Mediterranean and Italy, p. 519-547. I. Finetti ed., Elsevier.

Gogus, O. H., and R. N. Pysklywec (2008), Near-surface diagnostics of dripping or delaminating lithosphere, J. Geophys. Res., 113, B11404, doi:10.1029/2007JB005123

Improta, L., Iannaccone, G., Capuano, P., Zollo, A. and Scandone, P. (2000) Inferences on the upper structure of Southern Apennines (Italy) from seismic refraction investigations and subsurface data. Tectonophysics, 317, 273-297.

Keen, C.E., Beaumont, C., 1990. Geodynamics of rifted continental margins. In: Keen, Williams (Eds.), Chapter 9 in Geology of the Continental Margin of Eastern Canada. Geological Society of America, The Geology of North America, v. I-1, pp. 393–472.

Langston, C. A. (1979), Structure under Mount Rainier, Washington, inferred from teleseismic body waves, J. Geophys. Res., 84(B9), 4749–4762.

Latorre, D., Amato, A., Chiarabba, C. (2010) High-resolution seismic imaging of the Mw5.7, 2002 Molise, southern Italy, earthquake area: Evidence of deep fault reactivation. Tectonics, 29. DOI: Tc4014 10.1029/2009tc002595

Leahy, G. M., R. L. Saltzer, J. Schmedes (2012) Imaging the shallow crust with teleseismic receiver functions, Geophysical Journal International, 191, 2, 627-636 doi: 10.1111/j.1365-246X.2012.05615.x

Levin, V., L. Margheriti, J. Park, and A. Amato (2002), Anisotropic seismic structure of the lithosphere beneath the Adriatic coast of Italy constrained with mode-converted body waves, Geophys. Res. Lett., 29(22), 2058, doi:10.1029/2002GL015438.

Mariotti, G., and C. Doglioni (2000), The dip of the foreland monocline in the Alps and Apennines, Earth Planet. Sci. Lett., 181, 191–202, doi:10.1016/S0012-821X(00)00192-8.

McKenzie, D. P. (1970), The plate tectonics of the Mediterranean region, Nature, 226, 239– 243.

Miller, M. and N. Piana Agostinetti (2011), Erosion of the continental lithosphere at the cusps of the Calabrian arc: evidence from S receiver functions analysis, Geophys. Res. Lett., 38, L23301, doi:10.1029/2011GL049455.

Mooney, W. D., and T. M. Brocher (1987), Coincident seismic reflection/refraction studies of the continental lithosphere, A global review, Rev. Geophys., 25, 723-742.

Mooney, W. D., and R. Meissner (1992), Multi-genetic origin of crustal reflectivity: A review of seismic reflection profiling of the continental lower crust and Moho, in Continental Lower Crust, edited by D. M. Fountain, R. Arculus, and R. W. Kay, pp. 45-80, Elsevier Sci., New York.

Moretti, I., Royden, L., 1988. Deflection, gravity anomalies and tectonics of doubly subducted continental lithosphere: Adriatic and Ionian seas. Tectonics 7, 875–893.

Mostardini, F., and Merlini, S. (1986) Appennino centro-meridionale. Sezioni geologiche e proposta di modello strutturale. Mem. Soc. Geol. Ital., 35, 177^202.

Nicolai, C., and R. Gambini (2007), Structural architecture of the Adria platform-and-basin system, Boll. Soc. Geol. Ital., 7, 21–37.

Patacca, E. & Scandone, P. (1989) Post-Tortonian mountain building in the Apennines. The role of the passive sinking of a relic lithospheric slab. In: The Lithosphere in Italy (Ed. by A. Boriani, M. Bonafede, G.B. Piccardo & G.B. Vai), Acc. Naz. Lincei., 80, 156-176.

Patacca, E., P. Scandone, E. Di Luzio, G. P. Cavinato, and M. Parotto (2008), Structural architecture of the central Apennines: Interpretation of the CROP 11 seismic profile from the Adriatic coast to the orographic divide, Tectonics, 27, TC3006, doi:10.1029/2005TC001917.

Patella, D., Petrillo, Z., Siniscalchi, A., Improta, L. and Di Fiore, B. (2005) Magnetotelluric profiling along the CROP-04 section in the Southern Apennines. In: CROP PROJECT: deep seismic exploration of the Central Mediterranean and Italy, p. 263-280. I. Finetti ed., Elsevier.

Piana Agostinetti, N., and A. Amato (2009), Moho depth and Vp/Vs ratio in peninsular Italy from teleseismic receiver functions, J. Geophys. Res., 114, B06303, doi:10.1029/2008JB005899.

Piana Agostinetti, N., and A. Malinverno (2010), Receiver function inversion by trans-dimensional Monte Carlo sampling, Geophys. J. Int., 181(2), 858–872, doi:10.1111/j.1365-246X.2010.04530.x.

Piana Agostinetti, N., I. Bianchi, A. Amato, and C. Chiarabba (2011) Fluid migration in continental subduction: The Northern Apennines case study, Earth Planet. Sci. Lett., doi:10.1016/j.epsl.2010.10.039

Piccardi, L., F. Sani, G. Moratti, D. Cunningham, E. Vittori (2011). Present-day geodynamics of the circum-Adriatic region: An overview. J. of Geodynamics, 51 (2011) 81–89 doi:10.1016/j.jog.2010.09.002

949 Ridente, D. and F. Trincardi (2006). Active foreland deformation evidenced by
950 shallow folds and faults affecting late Quaternary shelf-slope deposits (Adriatic Sea,
951 Italy), Basin Research (2006) doi: 10.1111/j.1365-2117.2006.00289.x
952
953 Royden L., E. Patacca, and P. Scandone (1987) Segmentation and configuration of
954 subducted lithosphere in Italy; an important control on thrust-belt and foredeep-basin
955 evolution, Geology, 15(8):714-717.
956
957 Rudnick, R.L., and D.M. Fountain (1995), Nature and composition of the continental
958 crust, Review of Geophysics, 33,3, 267-309.
959
960 Scrocca, D., Carminati, E., Doglioni, C. (2005). Deep structure of the Southern
961 Apennines (Italy): thin-skinned or thick-skinned? Tectonics 24, TC3005.
962 doi:10.1029/2004TC001634.
963
964 Scrocca, D., C. Doglioni, F. Innocenti, P. Manetti, A. Mazzotti, L. Bertelli, L. Burbi,
965 and S. Doffizi (2003), CROP ATLAS—Seismic Reflection Profiles of the Italian
966 Crust, Mem. Descr. Carta Geol., Ital., vol. 62, 194 pp.
967
968 Scrocca, D., Doglioni, C., Innocenti, F., Manetti, P., Mazzotti, A., Bertelli, L., Burbi,
969 L., D'Offizi, S. (Eds.) (2003) CROP ATLAS – Seismic reflection profiles of the
970 Italian crust. Mem. Descr. Della Carta Geologica Italiana, Vol. LXII, Ist. Poligrafico e
971 Zecca dello Stato.
972
973 Spada, M., I. Bianchi, E. Kissling, N. Piana Agostinetti, and S. Wiemer, (2013).
974 Combining controlled-source seismology and receiver function information to derive
975 3-D Moho topography for Italy, Geophys. J. Int., doi:10.1093/gji/ggt148.
976
977 Speranza, F., and M. Chiappini (2002), Thick-skinned tectonics in the external
978 Apennines, Italy: New evidence from magnetic anomaly analysis, J. Geophys. Res.,
979 107(B11), 2290, doi:10.1029/2000JB000027.
980
981 Steckler M.S., Agostinetti N.P., Wilson C.K., Roselli P., Seeber L., Amato A. and
982 Lerner-Lam A. (2008). Crustal structure in the Southern Apennines from teleseismic
983 receiver functions, Geology, 36, n. 2, 155-158, doi: 10.1130/G24065A.1.
984
985 Stipcevic, J., H. Tkalcic, M. Herak, S. Markusic and D. Herak (2011) Crustal and
986 uppermost mantle structure beneath the External Dinarides, Croatia, determined from
987 teleseismic receiver functions, Geophys. J. Int. (2011) 185, 1103–1119 doi:
988 10.1111/j.1365-246X.2011.05004.x
989
990 Trippetta, F., C. Collettini, S. Vinciguerra, P.G. Meredith (2010) Laboratory
991 measurements of the physical properties of Triassic Evaporites from Central Italy and
992 correlation with geophysical data, Tectonophysics, 492,121–132.
993
994 Wedepohl K. H. (1995), The composition of the continental crust. Geochimica et
995 Cosmochimica Acta; 59:1217-1232.
996
997 Zhu, L., and H. Kanamori (2000), Moho depth variation in southern California from
998 teleseismic receiver function, J. Geophys. Res., 105, 2969–2980.

Figure captions

Figure 1. Location of seismic stations used in this study. Symbols' colours are indicative of previously published Moho depth estimates (from Piana Agostinetti and Amato, 2009), grey for stations not previously analyzed. White-filled circles show the position of the deep wells cited in the study. Background colours schematize simply the geology of Apulia; yellow for foredeep and Quaternary sediments, and green for carbonate units. Inset: map of the Italian region showing the Adria plate surrounded by the Apennines, Alps and Dinarides, and outcropping in the Apulia region. The box around Apulia includes the study area.

Figure 2. (a) A representative RF back-azimuthal sweep for station AMUR. The RF have been binned to increase the S/N ratio, see text for details. The green area around each bin represents the standard deviation computed in the binning procedure. (b) An example of the inversion technique for station AMUR. Left panel: posterior probability distribution (PPD) for *S*-velocity at depth, posterior mean vale for Vs (red line) and 2-σ confidence interval (dashed black lines). Central panel: PPD of the interface distribution at depth. Top right: the observed RRF compared with the mean synthetic RRF, showing an excellent match of the data. Bottom right: PPD of the number of seismic interfaces beneath the station: it broadly indicates how many isotropic layers compose the seismic structure beneath the station.

Figure 3. Results of the RF inversion at the twelve seismic stations analyzed in this study, from north to south. As in Figure 2b, for each station, the bottom panel shows the match between stacked observed radial RF and synthetic model; the top-left panel displays the posterior probability distribution of Vs at depth, with the mean value (red line) and 2-σ confidence interval (dashed lines); the top-right panel shows the distribution of Vs discontinuities at depth as computed by the inversion.

Figure 4. Comparison between velocity profile and interface distribution from RF and deep well logs: (above) station MRVN and Puglia-1 well (stratigraphy and sonic log), and (below) station SGRT and deep wells Gargano-1 and Foresta Umbra (stratigraphy). For station MRVN, it is interesting to note that, at the bottom of the high Vs region (between 5 and 6 km depth), the results of the RF inversion show a higher Vs standard deviation, related to a highly bimodal distribution of the Vs at such depth level. This features marks the bottom of the AMP, in agreement with the clear negative jump detected in the well sonic log at the base of the AMP Meso-Cenozoic marine sediments.

Figure 5. The structure of the Apulian platform for the 12 stations as obtained from the interpretation of our RF results. The colors are proportional to the computed Vs, according to the scale at the bottom. The lithological symbols are hypothesized on the

basis of the velocity profiles (see Section 3.1). When the results have too large uncertainties, no lithology symbol is used (e.g., ILCA).

Figure 6. Comparison of the 12 Vs profiles grouped by region (see text). From left to right: Gargano, Murge North, Murge South, Salento. There are striking similarities for almost all the stations, with some difference for a few of them, explained in the text.

Figure 7. Histograms of the Vs discontinuity distributions in the lower crust – upper mantle depth range for all the 12 stations, as obtained by the RF inversion. The red line is the best-matching gaussian curve that fits the distribution, and the value used for the Moho depth is the mean of such gaussian curve (see Table 1 for details).

Table 1. Moho depth estimates. From: (A) this study; (B) Piana Agostinetti and Amato (2009); (C) Miller and Piana Agostinetti (2011); (D) Spada et al. (2013). For (C), error on Moho depth estimates are as large as 10 km, due to the low-frequency content of S-waves (Miller and Piana Agostinetti, 2012). NRF indicates the number of high S/N ratio RF selected for each station.

(A)	(B)	(C)	(D)					
	NRF	Depth (km)	σ (km)	Depth (km)	σ (km)	Depth (km)	Depth (km)	σ (km)
AMUR	153	30	3	29	1	29	37	6
CRBB	45	30	3	31	2	-	32	3
ILCA	42	30	4	31	4	-	28	6
MATE	79	29	4	-	-	-	-	-
MESG	39	27	3	-	-	-	-	-
MRVN	231	26	3	30	4	26	27	6
MSAG	184	31	4	27	2	24	30	3
NARD	25	29	3	30	2	-	28	10
NOCI	137	30	4	-	-	28	-	-
SCTE	101	30	4	32	5	26	30	3
SGRT	146	30	4	30	2	22	30	10
SRRN	23	31	3	33	3	-	-	-

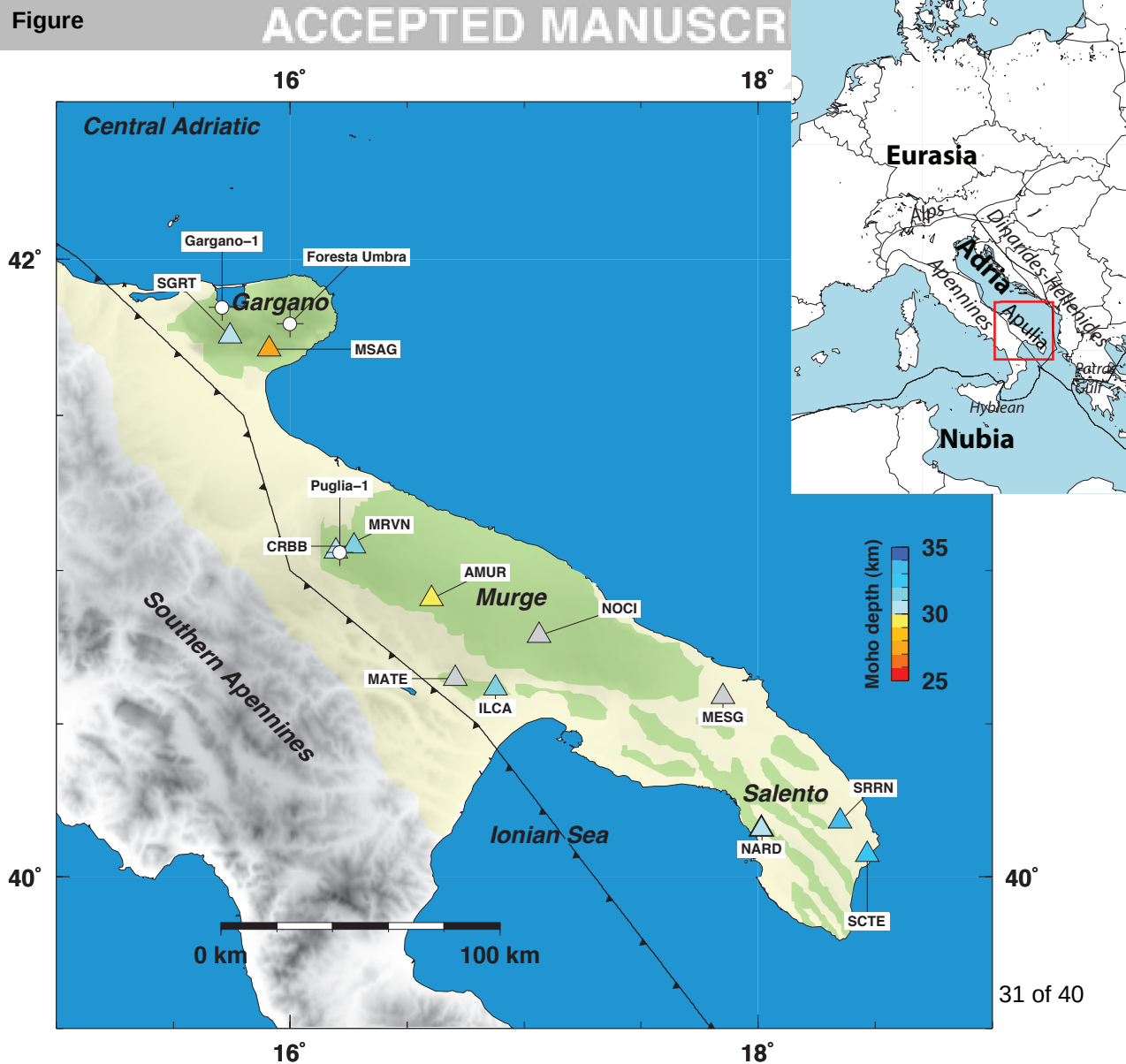

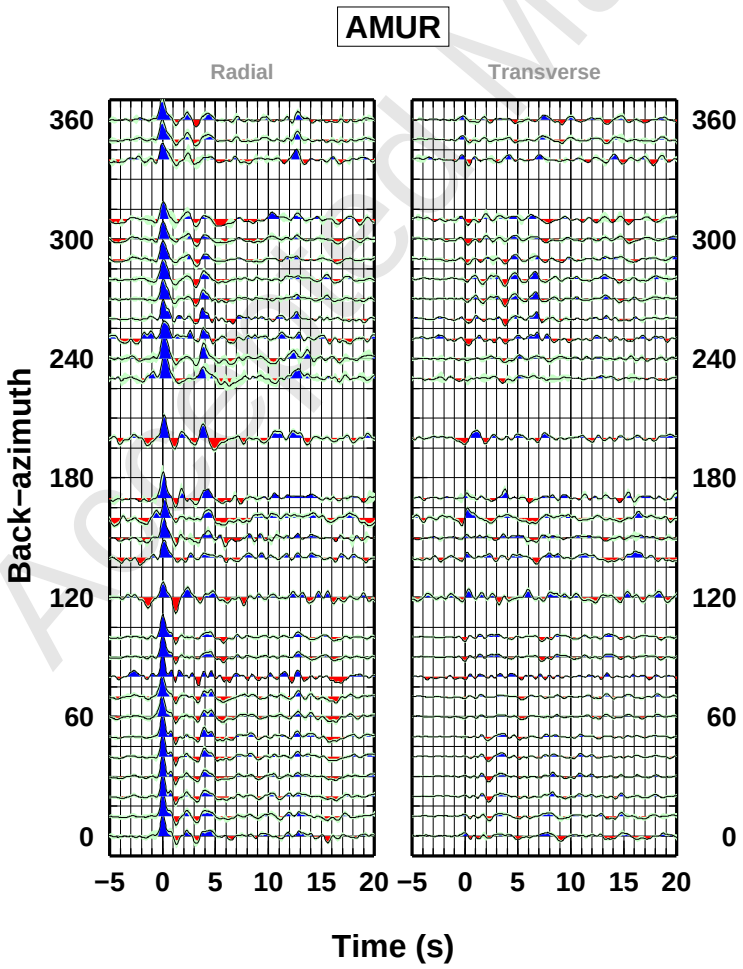

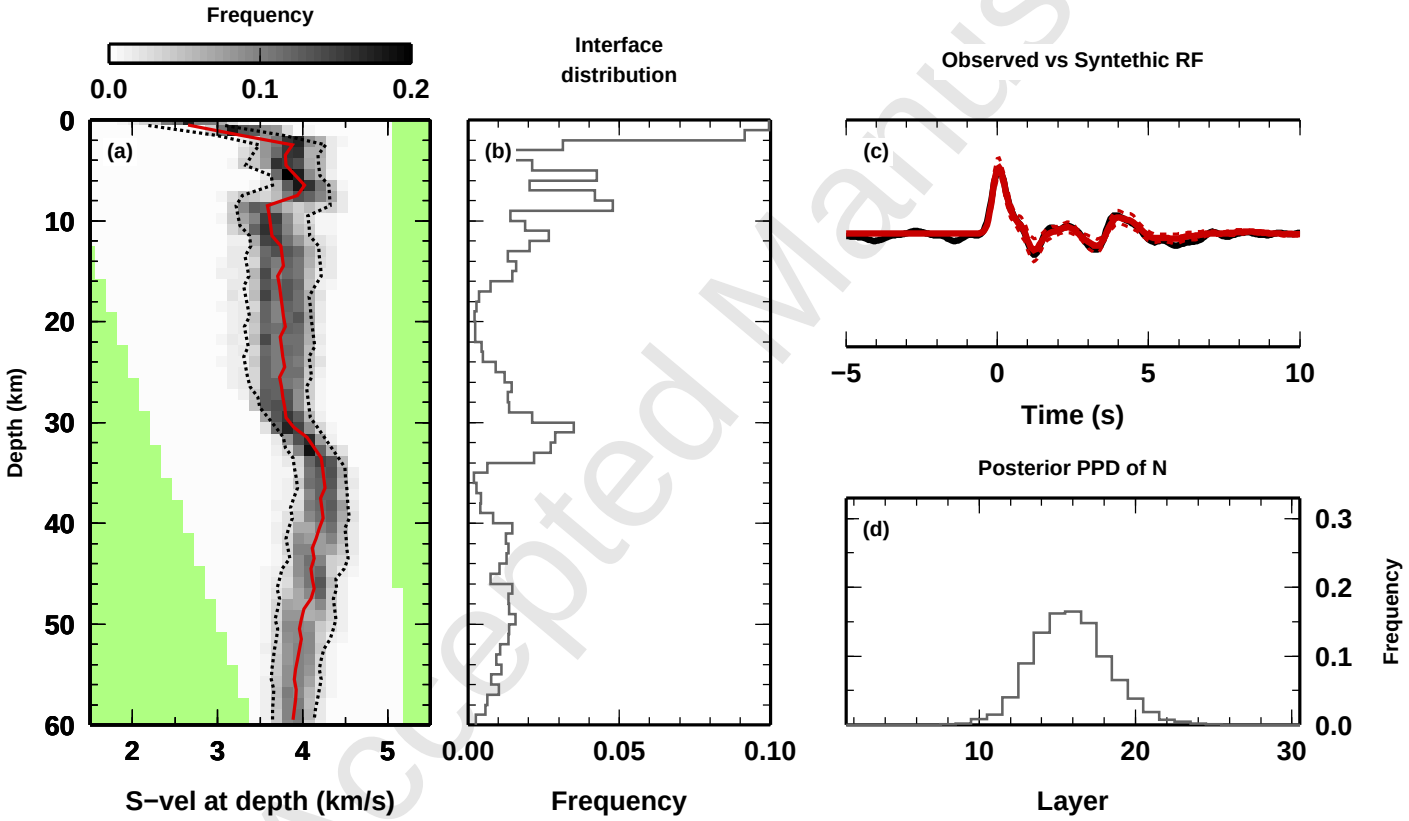

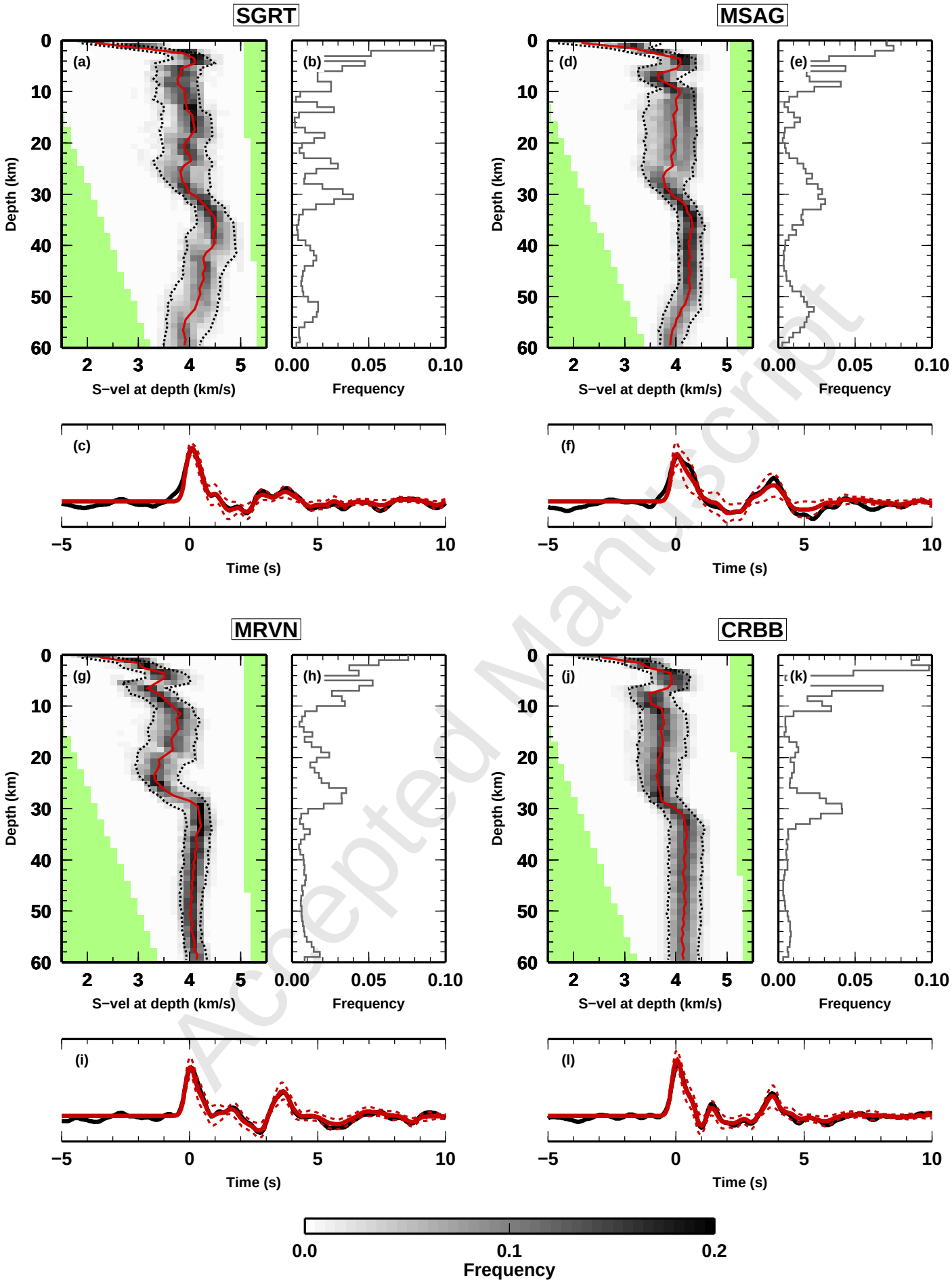

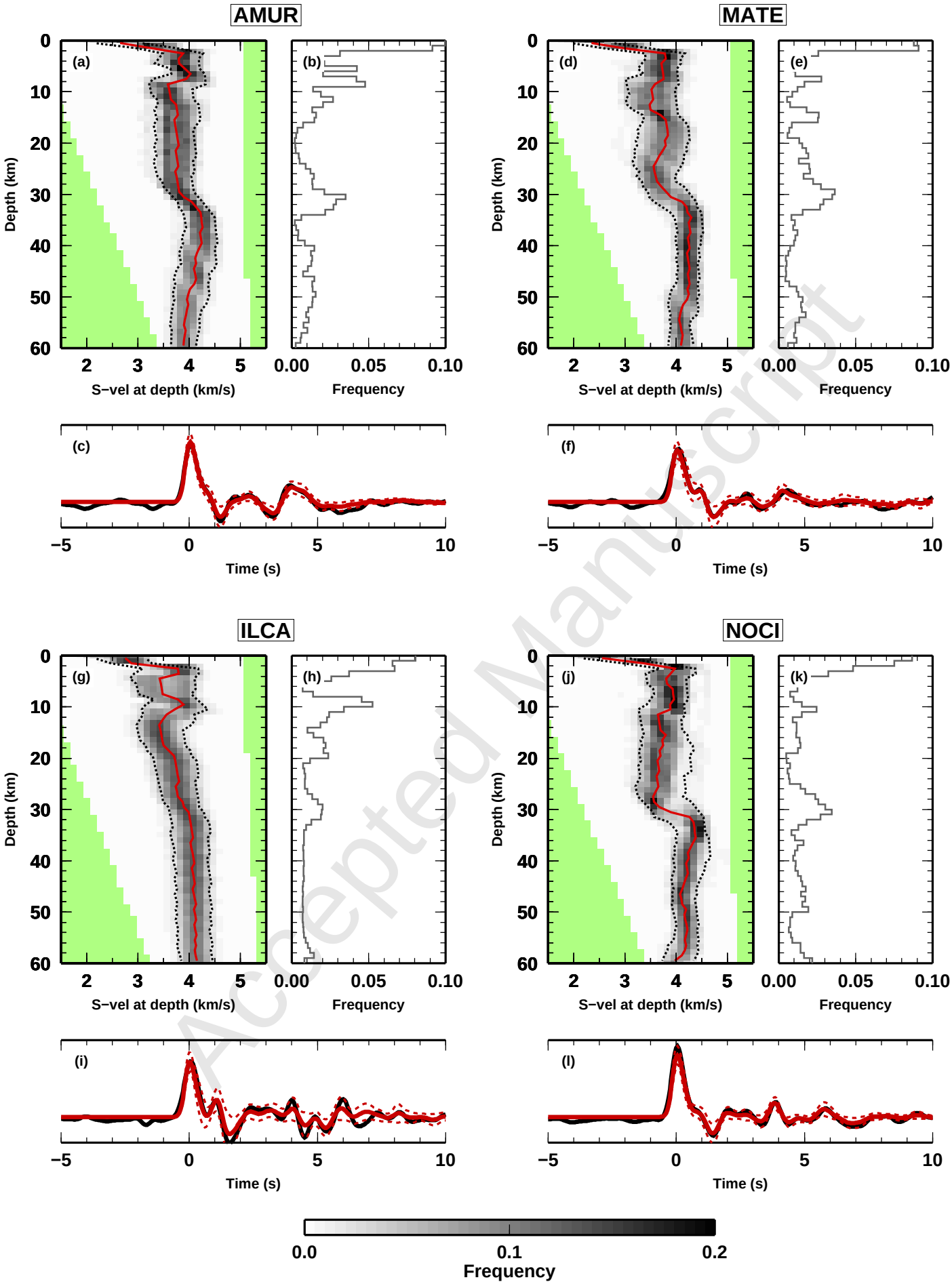

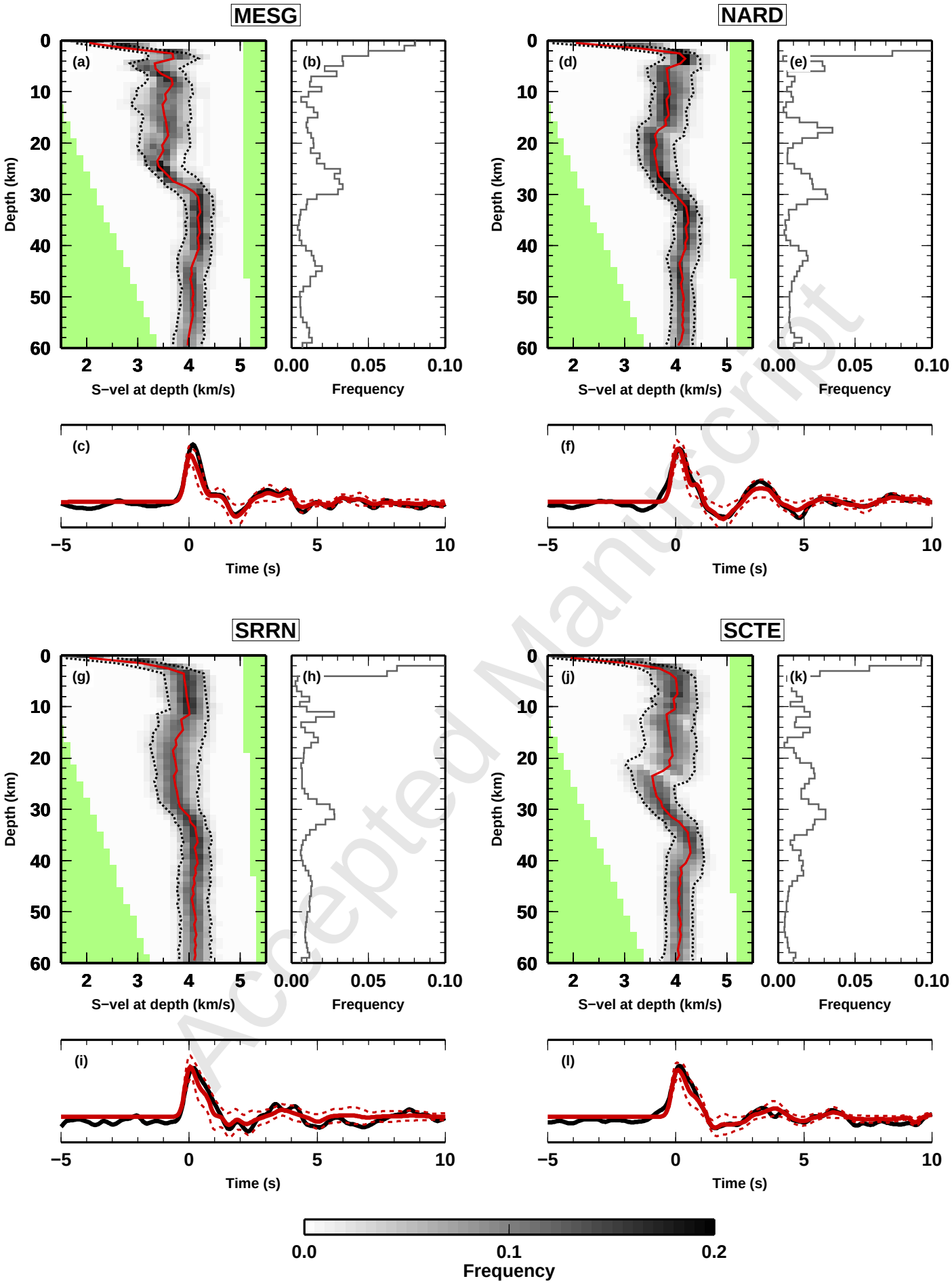

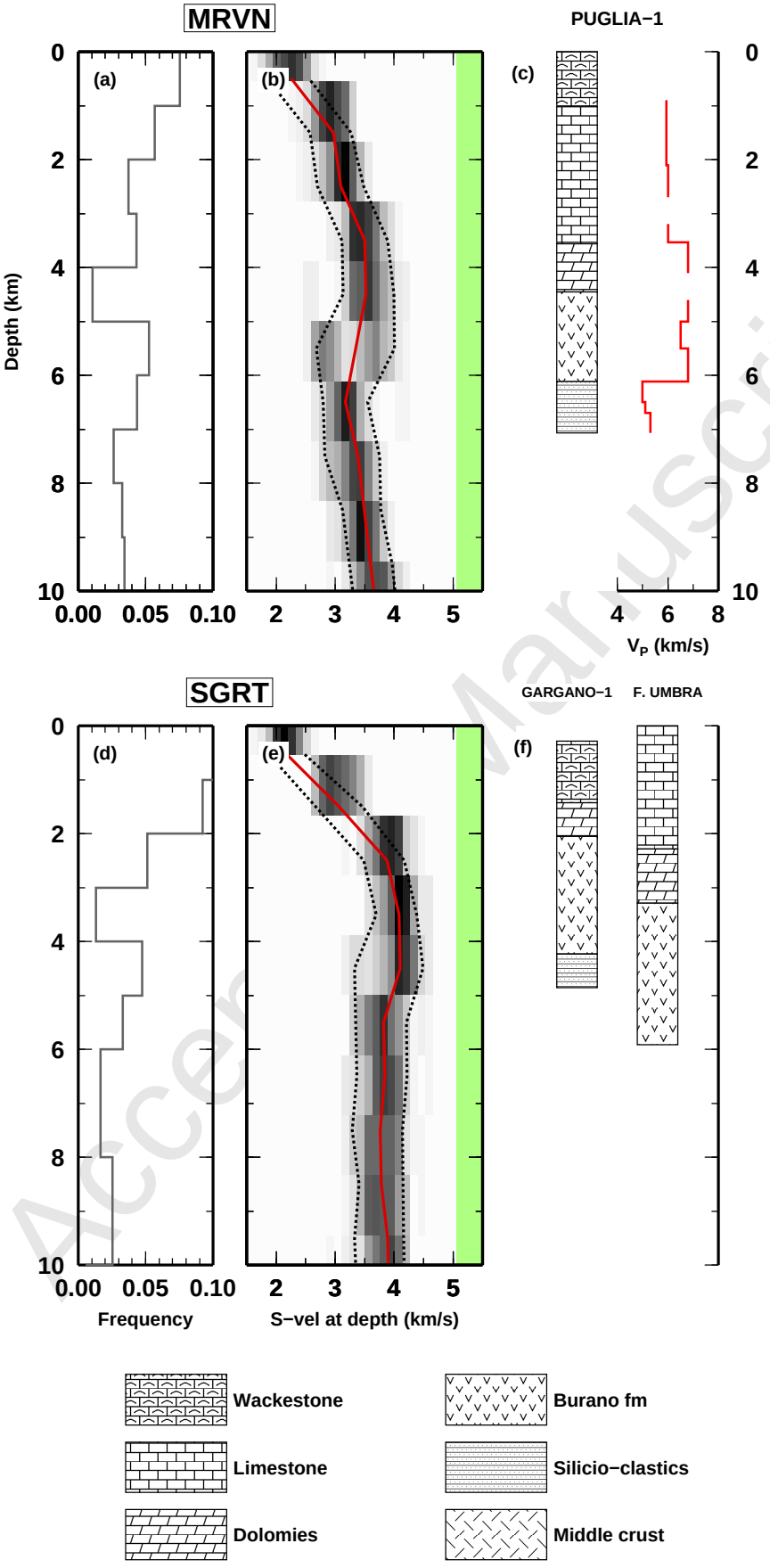

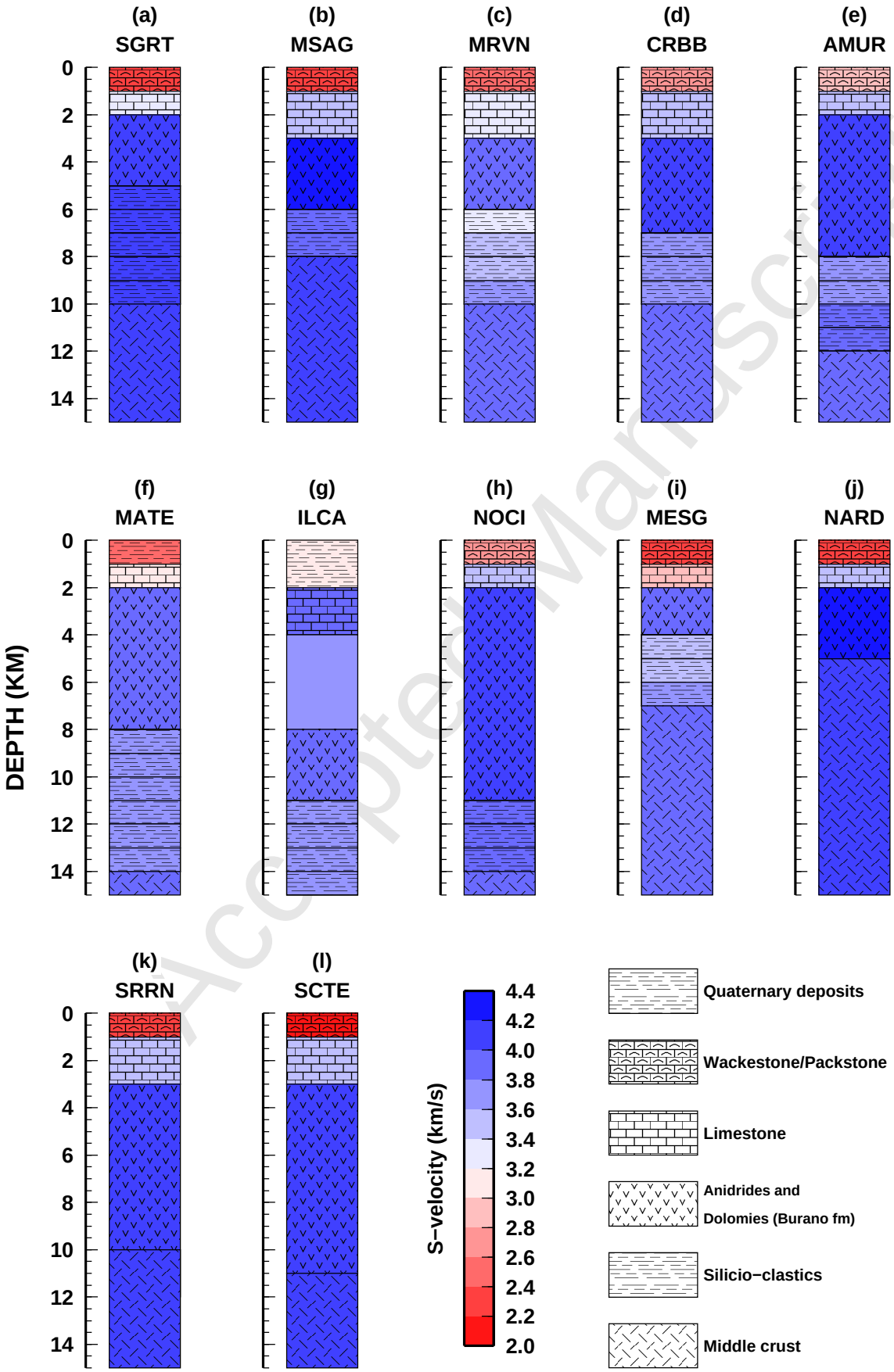

Figure